

Fatigue characterization of a spheroidal graphite cast iron under ultrasonic loading

Q. Y. WANG

Department of Civil Engineering & Mechanics, Sichuan University, Chengdu 610065, People's Republic of China
E-mail: wangqy@scu.edu.cn; wangqy2000@hotmail.com

C. BATHIAS

Department of Mechanical Engineering, ITMA-CNAM, Paris 75003, France

Due to its useful combination of high tensile strength, good wear resistance and ductility, spheroidal graphite (SG) cast iron is widely used for automotive structural applications. The required design lifetime of many components (suspension arms, gears, crankshafts, etc.) often exceeds 10^9 cycles [1–4]. Although many fatigue data of SG cast irons have been published, most experimental data in the literature have been limited to fatigue lives up to 10^7 cycles. It is well known that many materials do not exhibit a conventional endurance limit in S-N curves between 10^6 and 10^7 cycles [1–8]. Fatigue failure could occur beyond 10^7 cycles. It is therefore important to realize the risk of using an arbitrary cut-off value of 10^6 (or 10^7) cycles to establish the fatigue limit.

In general, fatigue crack initiation is understood to occur on the specimen surface owing to the irreversible process of extrusions and intrusions through slip deformation. Many materials, however, clearly exhibit two kinds of fatigue initiation. One is at the specimen surface, and the other is in the specimen interior. Subsurface crack initiation is dominant in the long-life range, while the surface fatigue crack initiation occurs in high-peak stress tests and in short-life tests [4–8]. To clarify the crack initiation mechanism in very high cycle fatigue, a SG cast iron was tested between 10^5 and 10^{10} cycles using a piezoelectric fatigue test machine operating at 20 kHz. By using scanning electron microscopy (SEM), the crack initiation behavior has been examined.

It is well known that heat dissipated during cyclic loading is sensitive to the fatigue state of material [9]. Heating of specimens loaded at ultrasonic frequencies is caused by the absorption of ultrasonic energy. In this work, advanced infrared thermography is used to evaluate the evolution of temperature of specimen during fatigue testing.

The material used in this study is a spheroidal graphite cast iron with a pearlite content of 5% (vol.). The volume fraction of nodules is 0.1, with a mean size of $15 \mu\text{m}$ and a ferrite grain size of $50 \mu\text{m}$. The bulk matrix exhibits a homogeneous distribution of nodules in the ferrite matrix (Fig. 1). The mechanical properties and the chemical composition are shown in Tables I and II, respectively.

Hourglass-shaped specimens designed to resonate longitudinally at 20 kHz were provided by Renault.

The specimen has a gauge length of 30.0 mm, a gauge diameter of 10.0 mm, a maximum section diameter of 20.0 mm, and a continuous radius of 25.0 mm. The total resonance length of the specimen calculated using an analytical method [4, 6] is 88.7 mm. The specimen gauge surfaces were mechanically polished before testing.

Fatigue testing was carried out in a piezoelectric resonance system operating at 20 kHz with stress ratios of $R = -1$ and $R = 0$. The testing facility has been described in detail elsewhere [4–6]. The vibration loading amplitude was controlled during the test. The specimens were cyclically loaded until failure or up to 10^9 cycles as run-out. Some specimens of the SG cast iron were used for conventional fatigue tests at Renault with a loading frequency of 25 Hz.

Results of high cycle fatigue S-N curves of the SG cast iron with $R = -1$ and $R = 0$ are shown in Fig. 2a and b. The result shows no noticeable frequency effect on the fatigue behavior. For zero mean stress $R = -1$, the high frequency (20 kHz) fatigue data closely matched the conventional frequency (25 Hz) test results between 10^5 and 10^7 cycles, and for $R = 0$, the fatigue strength obtained by the piezoelectric fatigue machine seems to be slightly higher than that given by conventional fatigue loading. The specimens continued to fail over 10^7 stress cycles.

The fracture surfaces of tested specimens were investigated by SEM. The material clearly exhibits two kinds of crack initiation (Fig. 3). One is at the specimen surface, and the other is in the specimen interior. Subsurface crack initiation is dominant in the long-life range ($> 10^7$ cycles), while the surface fatigue initiation occurs in short-life tests. The observations show that the crack initiation sites were at microshrinkage cavities in the subsurface of the specimens (Fig. 3b and c). There is a definite stress (or cycle) range where the initiation location changes from the surface to the interior, i.e., at 10^7 cycles.

Fatigue loading of a material causes a temperature change, due to energy dissipation caused by hysteretic effects and thermoelasticity [9]. Both the material and fatigue loading condition have a decisive influence on the heat dissipation. Infrared thermography techniques have been shown to be highly effective methods for determining the characteristic changes in the heat dissipation during mechanical loading [9, 10].

TABLE I Mechanical properties

Elastic modulus E (GPa)	Density ρ (kg/m ³)	Ultimate tensile strength σ_T (MPa)	Hardness (HV)
178	7100	510	184

TABLE II Chemical composition (wt%)

C	Si	Mn	Cu	Mg	P	S	Ni
3.45	3.21	0.13	0.02	0.03	0.03	0.02	0.59

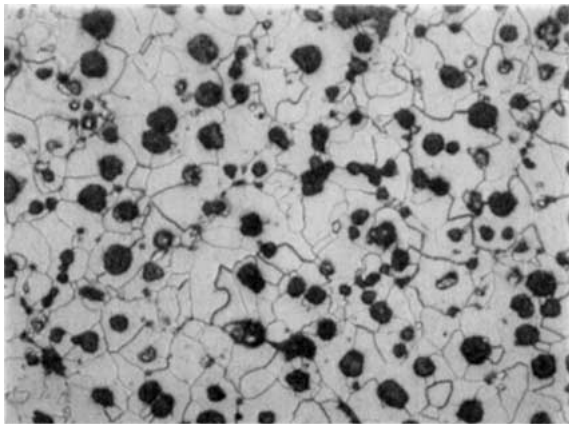
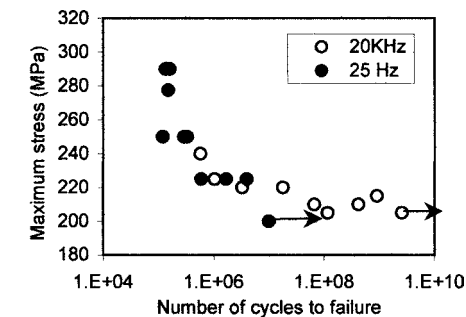
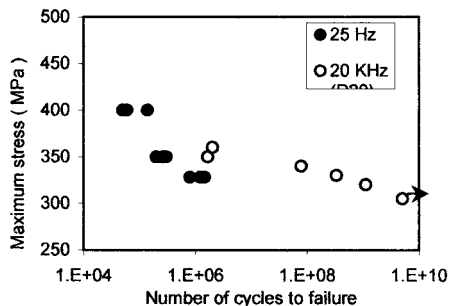


Figure 1 Microstructure of the SG cast iron.



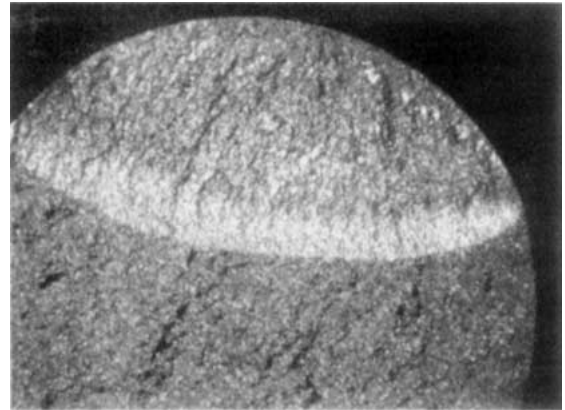
(a) R=-1



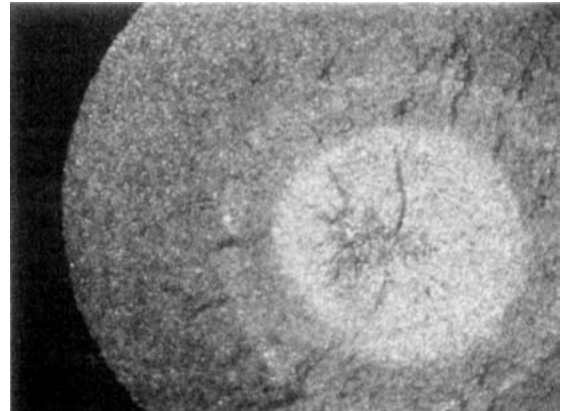
(b) R=0

Figure 2 S-N curves for the SG cast iron.

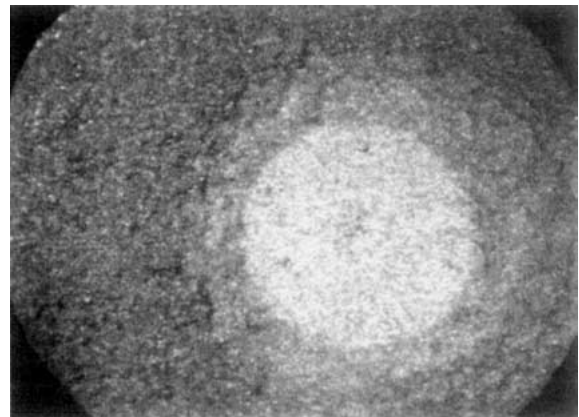
The temperature variation during fatigue testing was measured with infrared thermography. The temperature curve of specimens during a test consists of two zones (Fig. 4): Initially, a steep rise in temperature occurs up to 10⁶ cycles, then a maximum temperature is attained which depends on the stress amplitude. The curve then becomes almost horizontal. This may be interpreted as



(a) $N_f = 3.3 \times 10^6$ cycles, $R = -1$



(b) $N_f = 6.7 \times 10^7$ cycles, $R = -1$



(c) $N_f = 7.9 \times 10^7$ cycles, $R = 0$

Figure 3 SEM micrographs of the fatigue fracture surfaces of the SG cast iron: (a) crack initiated at the surface and (b)–(c) the crack origins are subsurface microshrinkage cavities.

an adaptation of the material to the internal friction. A possible explanation of the adaptation is that the dissipation of a part of the ultrasonic energy is due to interior crack initiation.

Once the maximum temperature is reached, there is no substantial decrease in the temperature range particularly for a low number of cycles to failure where the crack initiation starts on the surface. A short fatigue lifetime is related to a higher increase of temperature. When the initiation is in the interior ($> 10^7$ cycles) of the specimen, the temperature change during the process of fatigue damage is much less significant, and the maximum temperature could correspond to the formation of microcracks.

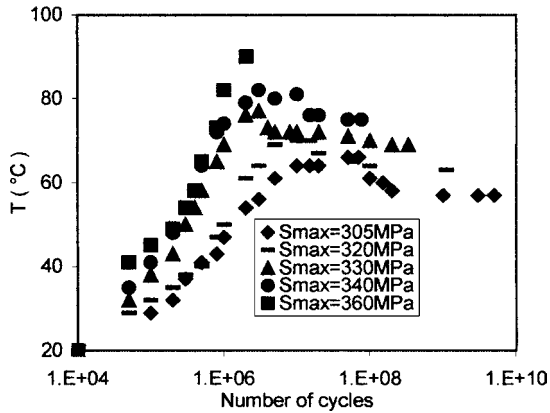


Figure 4 Detected temperature distributions during fatigue process.

Very good agreement is found with the results obtained from ultrasonic fatigue tests (20 kHz) and conventional tests (25 Hz). The most noticeable conclusion was that specimens continued to fail beyond 10^7 cycles. It is therefore important to realize the risk of using an arbitrary cut-off value of 10^6 (or 10^7) cycles to establish the fatigue limit.

The SG cast iron exhibits two kinds of crack initiation. One is at the specimen surface, and the other is in the specimen interior. A surface-subsurface transition in crack initiation location has been described at 10^7 cycles.

The temperature variation during fatigue testing was measured with infrared thermography. The results show

potential applications of this technique in quantitatively evaluating fatigue crack initiation and propagation.

Acknowledgments

This work is supported in part by the Excellent Young Teachers Program of MOE, China.

References

1. Q. Y. WANG, C. BATHIAS, N. KAWAGOISHI and Q. CHEN, *Int. J. Fatigue* **24** (2002) 1269.
2. Q. Y. WANG, J. Y. BERARD, A. DUBARRE, G. BAUDRY and C. BATHIAS, *Fatigue Fract. Engng. Mater. Struct.* **22** (1999) 667.
3. Q. Y. WANG, J. Y. BERARD, S. RATHERY and C. BATHIAS, *ibid.* **22** (1999) 676.
4. *Idem.*, *Rev. Metall.* **96** (1999) 221.
5. C. BATHIAS, *Fatigue Fract. Engng. Mater. Struct.* **22** (1999) 559.
6. Q. Y. WANG, Ph.D Thesis, Ecole Centrale Paris, France, 1998.
7. Y. MURAKAMI, M. TAKADA and T. TORIYAMA, *Int. J. Fatigue* **20** (1998) 661.
8. K. SHIOZAWA and L. LU, *Fatigue Fract. Engng. Mater. Struct.* **25** (2002) 813.
9. N. G. MEYENDORF, H. ROSNER and V. KRAMB, *Ultrasonics* **40** (2002) 427.
10. M. P. LUONG, *Mech. Mater.* **28** (1998) 155.

Received 10 April
and accepted 31 July 2003